Numerical Investigation of Hybrid Savonius-Darrieus Vertical Axis Wind Turbine at Low Wind Speeds

Numerical Investigation of Hybrid Savonius-Darrieus Vertical Axis Wind Turbine at Low Wind Speeds

Hesam Eftekhari[1, a)], Abdulkareem Sh Mahdi Al-Obaidi[1, b)], and Sucharita Srirangam[2,c)]

[1] School of Computer Science and Engineering, Taylor's University, Malaysia
[2]School of Architecture, Building & Design, Taylor's University, Malaysia

[a)]Corresponding author: Hesam.Eftekhari@sd.taylors.edu.my
[b)] Abdulkareem.Mahdi@taylors.edu.my
[c)] Sucharita.Srirangam@taylors.edu.my

Abstract. The need for electricity on the Earth is increasing day by day, and this requires building more electric power plants where most of the power plants cause CO2 emission which would increase the global warming. Using wind energy as one type of renewable energies, would contribute to reduce the global warming. In countries such as Malaysia where the average annual wind speed is 2-2.5 m/s using wind energy is a challenge because of the low wind speed. However, using a hybrid Savonius-Darrieus vertical axis wind turbine in low wind speed areas, the performance of the wind turbine may increase, and the starting rotation speed will decrease. This research aims at a comprehensive study on a hybrid Savonius-Darrieus wind turbine with helical Savonius rotor combined with helical and straight bladed Darrieus rotor. In this research, a base model with the name of Model Base was generated and two models with new configurations were generated in SOLIDWORKS. A numerical studies and simulation were conducted on these three designs using Ansys Fluent to identify the more suitable combination for low wind speed areas. Based on the obtained result hybrid Savonius-Darrieus with helical Savonius rotor and helical Darrieus rotor were found to be the most suitable combination because of their stable aerodynamic performance throughout a full rotation. Best performance for these models was found to be at 0.45 TRS with maximum torque and power coefficients of 0.68 and 0.306 respectively.

1. Introduction

Living on the Earth for humans is going to be harder and uncomfortable due to global warming. This global warming is because of the molecular structure of the greenhouse gasses, which make them be able to trap heat in the atmosphere and, after that, transfer those heat to the surface of the Earth, and as a result, it would further warm the Earth [1]. Based on the collected data in Enerdata for Global Energy Statistical Yearbook 2021 [2] in which on this website all the collected data are from all the local power generator companies all over the world, CO_2 emissions are increasing almost every year globally while CO_2 is one of the most effective gasses of greenhouse effect [3].

Nowadays everything is powered by electricity, and each year the human need for electricity is increasing. Based on the data, which was gathered by IEA, the majority of electricity production is by coal. Coal is a fossil fuel, and when it burns to do the processing of producing electricity, and while it burns, it produces carbon emissions, and at last, it would cause global warming [4]. One of the ways to produce electricity is by using renewable energy which the most popular types are, solar energy, wind energy, hydro energy, tidal energy, geothermal energy, and biomass energy. By using these energies which are also known as green energy, the carbon emissions would reduce on the Earth. Among the renewable resources, wind energy and solar energy are well known. But wind energy is a better source of renewable energy as solar energy highly depends on sunlight. So, using wind energy is more cost-effective compare to other renewable resources [5]. That is the reason there have been so many developments in wind energy in the past decades. In Malaysia and many other ASIAN countries, the average annual wind speed is less than

3m/s. For many islands and places in these low wind speed regions, the electric power transmission is not justifiable with the tropical climate, which is almost cloudy. Since solar energy depends on sunlight, it is impossible to make solar energy the primary source of energy [6]. The kinetic energy generated from the movement of atmospheric air is called wind energy [7] and to harvest energy from wind, wind turbines are being used which are mainly categorized as Horizontal Axis Wind Turbines (HAWT) and Vertical Axis Wind Turbines (VAWT) and they are presented in figure 1.

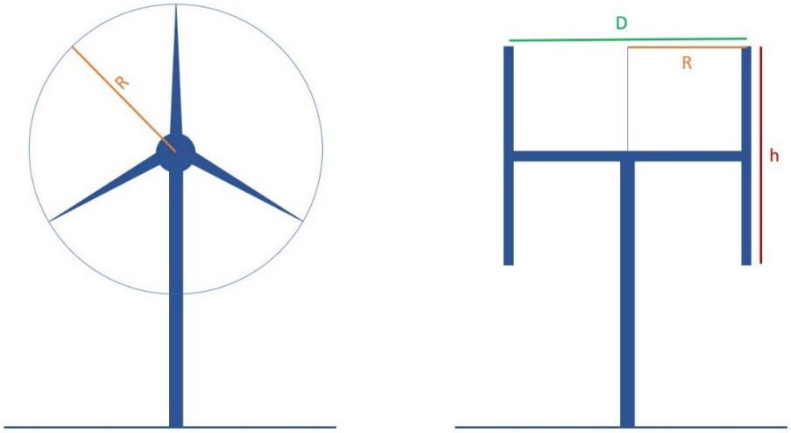

Figure 1. HAWT on left and VAWT on right

The very first step for using wind turbine in any area is to study and measure the wind speed of that area, because the wind speed is one of the main factors that directly effect on the output power of a wind turbine [8]. The wind power or available power for a wind turbine is calculated using Eq. (1) used:

$$P_w = \frac{1}{2} \times \rho \times A \times V^3 \tag{1}$$

where ρ is air density (kg/m^3), A is rotor swept area (m^2), V is wind velocity (m/s) [9]. Yet there is a slight difference between calculating the power in the wind for HAWT and VAWT which are expressed in Eqs. (2) and (3) respectively:

$$P_w = \frac{1}{2} \times \rho \times \pi \times R^2 \times V^3 \tag{2}$$

$$P_w = \frac{1}{2} \times \rho \times h \times D \times V^3 \tag{3}$$

where h is the height of turbine blades (m), R is the radius of the HAWT (m) and D is the diameter of the VAWT (m) he captured mechanical energy by the wind blades converts to electrical energy via wind generators. This conversion has an efficiency, which is determined by Gearbox efficiency, Generator efficiency, Electrical efficiency, and the power coefficient. It should be noted that, C_p, the power coefficient, with ideal conditions has a maximum value of $C_{p_{max}} = 0.5926$ which is also known as the Betz Limit [10]. The total power conversion efficiency from wind to electricity can be calculated from Eq. (4) [11].

$$\eta_t = C_p \times \eta_{gear} \times \eta_{gen} \times \eta_{ele} \tag{4}$$

So, the effective power output from a wind turbine is determined using Eq. (5).

$$P_{eff} = C_p \times \eta_{gear} \times \eta_{gen} \times \eta_{ele} \times P_w = \eta_t \times P_w \tag{5}$$

To increase the wind power (P_w), since the air density value is almost the same, either location must be selected where it has higher wind speed or to increase the rotor's swept area. On the other hand, to increase the total power conversion efficiency, either the power coefficient, gearbox efficiency, generator efficiency, or electrical efficiency has to be increased. Therefore, by implementing a suitable design for low wind speed with a higher power coefficient, it is possible to increase the effective output

power of WTs at low wind speed. Overall, this would help reduce the usage of electrical power plants, leading to reducing global warming.

Darrieus rotors have good aerodynamic performance but usually are not self-starting, while the Savonius rotors are self-starting but have low aerodynamic performance because the Savonius rotors will function with drag forces. A combination of them or in other words hybrid Savonius-Darrieus rotor will help to solve the self-starting challenge for the Darrieus rotor and low aerodynamic performance of the Savonius rotor [12].

Previous studies show that helical Savonius rotor with the full circular end plates has 36% higher power coefficient compared to one without end plates. End plates deflect more air into the helical buckets where increase the torque [13, 14]. Savonious rotor with helical has a better performance compared to the conventional model as it doesn't generate negative torque during the rotation [15, 16].

Previously, researches and developments have been done on designing micro wind turbines for low wind speed areas [17–19]. But the challenge with the micro wind turbines is that they produce low output power. However, using micro wind turbines is not the way. This challenge can be solved by implementing an efficient hybrid Savonius-Darrieus VAWT configuration.

This research aims to improve the potential of hybrid VAWTs to produce higher output power from the WT at low wind speeds. By implementing two different hybrid Savonious-Darrieus VAWT. NACA 0015 was selected as the airfoil blade of the Darrieus rotor, as it shows a better performance with higher power coefficient among the 4 most common airfoils used on VAWTs. Three-bladed Darrieus rotor with helical and straight bladed models were selected as it was found that three-bladed Darrieus rotors perform better than the two-bladed ones [20].

The numerical analysis of this paper was done by 3D computational fluid dynamic (CFD) simulation by using Ansys workbench to gather the torque coefficient C_q.

2. Research Methodology

2.1 3D Geometry Modelling

The base design parameters for the initial design of this study are shown in Table 1 [21]. It is a combination of straight Darrieus rotor and conventional Savonius rotor. The base model was generated based on these parameters and named as Model Base.

Then two new hybrid Savonius configuration were generated for this study with the same configurations as the Model Base with minor adjustments to improve the performance of the wind turbine at low wind speed. The following two models were generated using SolidWorks software:

- Helical Savonius rotor with helical Darrieus rotor with NACA 0015. (Model 1)
- Helical Savonius rotor with straight-bladed Darrieus rotor with NACA 0015. (Model 2)

All models were scaled down to 1/7 of the original size to be able to place them inside Taylor's wind tunnel test section to minimize the interference effect of the test section wall. The scaled models were used for simulations as well to reduce the computational time. Model Base, Model 1 and Model 2 are presented in figures 2, 3 and 4 respectively.

Table 1. Base design parameters of this study (Model Base)

	Darrieus	**Savonius**
Blade profile	NACA 0021	NA
Chord length (m)	0.0858	NA
Height (m)	1.45	1
Rotor Diameter (m)	1.03	0.5
Solidity	0.5	NA
Number of blades	3	2
Blade overlap ratio	NA	0.25
Endplate thickness (m)	NA	0.01
Blade thickness (m)	NA	0.01
Shaft diameter of rotors	0.014	
Setting angle between the rotors	0º	

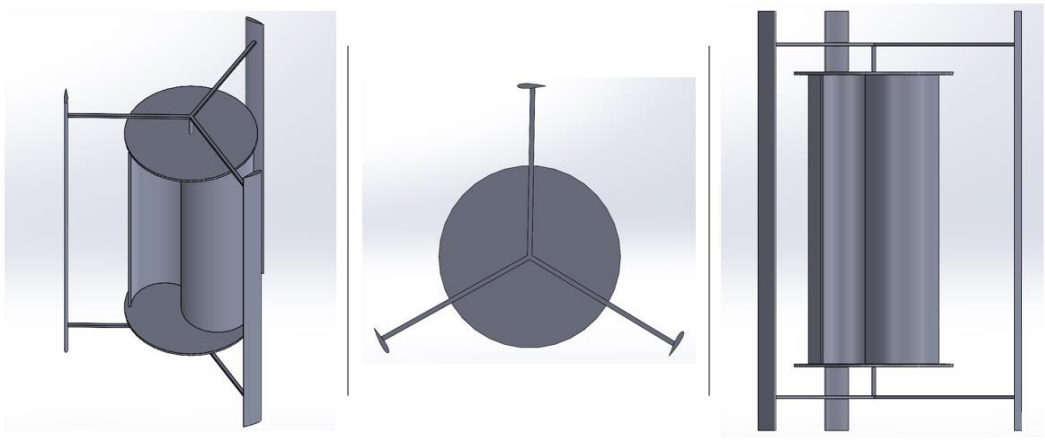

Figure 2. Model 1 isometric on left, top on middle, and side view on right

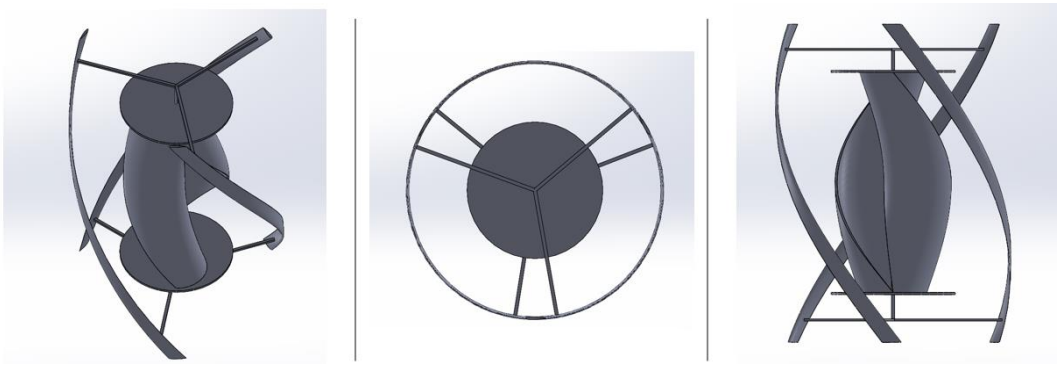

Figure 3. Model 1 isometric on left, top on middle, and side view on right

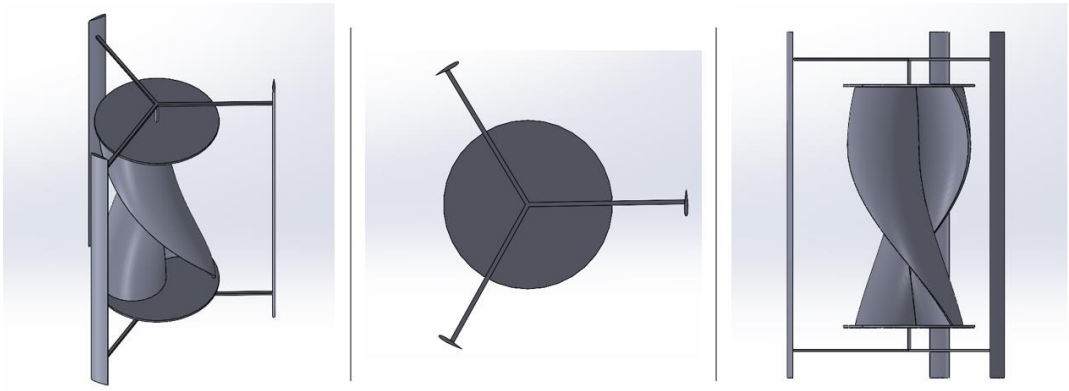

Figure 4. Model 2 isometric on left, top on middle, and side view on right

2.2 Numerical Method

2.2.1 Model and Meshing Setup. Computational fluid dynamics (CFD) is one of the most applicable numerical methods. Numerical simulations of this paper are conducted in ANSYS FLUENT. Firstly, a boundary domain was designed in ANSYS DesignModeler around the models to simulate the airflow along the geometry. Inlet, outlet, and turbine body were defined to emulate real life condition as best as possible. To be time efficient for computational simulation. Shahrooz [22] C-Type grid topology is used to generate the mesh around the turbine models. Figure 5 shows the boundary domain geometry which was used for all wind turbine models which contains of outer boundary, inner boundary (the cylinder boundary around the wind turbine) and the wind turbine.

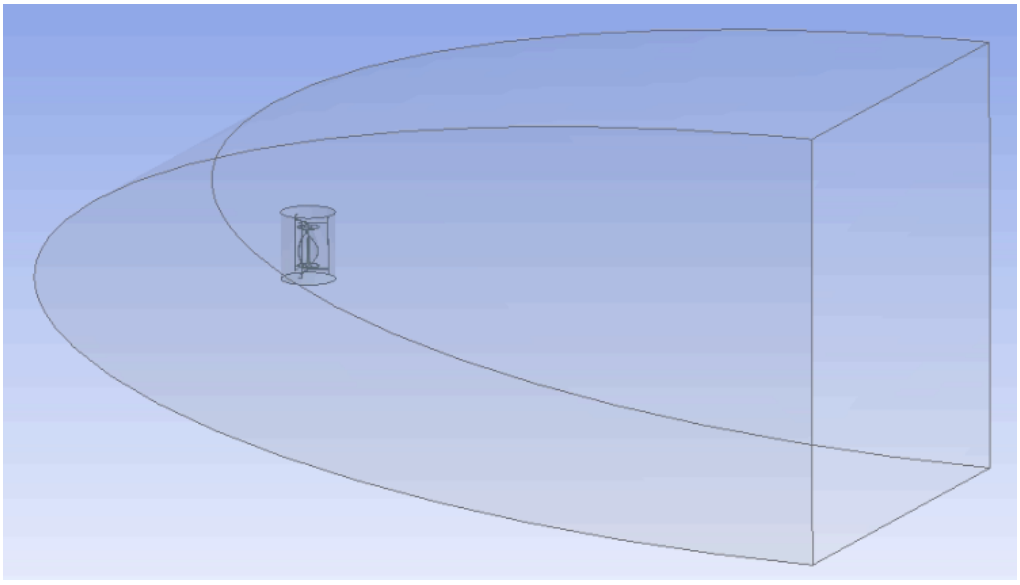

Figure 5. Boundary domain for wind turbines

A fine mesh is required to achieve an accurate simulation result. Figure 6 shows the generated mesh for Model 2 by using Edge sizing on the edges of the wind turbines and surface inflation first layer of thickness with 15 layer and 1.2 growth rate were used to generate a fine and time efficient mesh. Table 2 present the mesh methods and locations that were used. Figure 7 presents the generated mesh for the inner boundary. Same boundary and meshing methods were used for Model Base and Model 1. Table 2 present the mesh methods and the locations that they were used.

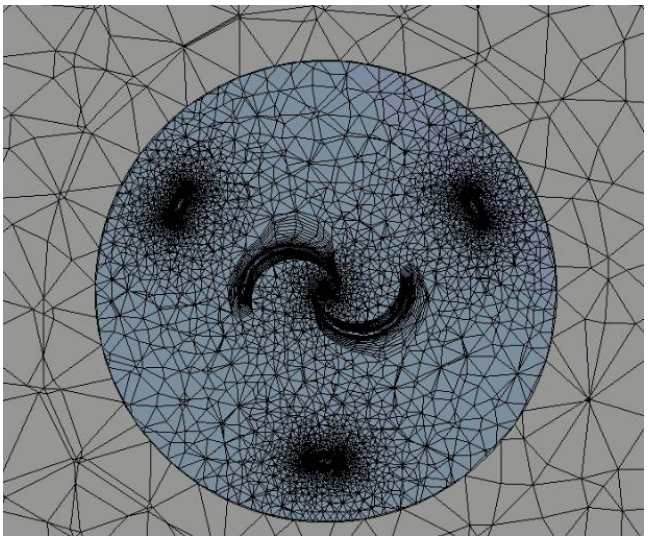

Figure 6. Generated mesh for Model 2

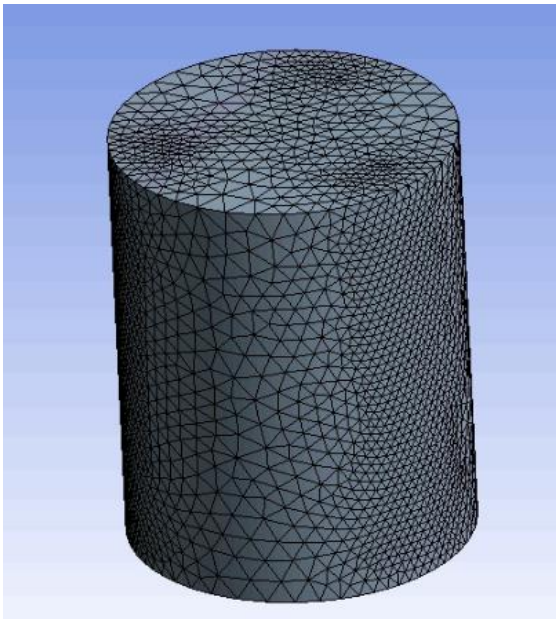

Figure 7. Generated mesh for the inner boundary

Figure 6 shows the sliced (half) of the geometry. As it can been from figure 6 the inflation method was used to create multiple layers of mesh around the edges of the wind turbine to have the mesh more concentrated around the wind turbine model and to increase the efficiency of the mesh around the model.

Table 2. Mesh characteristics

	Edge sizing (edges of airfoils)	Edge sizing (Height of Darrieus Blades)	Edge sizing (central shaft)	Edge sizing (edges of Savonius rotor)	Inflation	Elements
Model Base	0.001	0.008	0.008	0.005	0.001	5745919
Model 1	0.001	0.005	0.008	0.005	0.001	7093560
Model 2	0.001	0.008	0.008	0.005	0.001	6152934

2.2.2 Numerical Setup. The flow on this study is considered incompressible because the Mach number is less than 0.3. Properties of the fluid are presented on Table 3. As it was investigated by Mohamed and Shubham [23,24], Realizable k-ε turbulence model with standard wall function is selected for this study since it is time efficient and valid for wing simulation at low speeds. To compare the models with each other and to compare the numerical and experimental result, same Reynold number (Re) must be used. On this study Re $\approx 8.6 \times 10^5$ is used. The fluid properties for the simulation are presented in Table 3.

Table 3. Simulation fluid properties assumptions.

Fluid	Temperature (K)	Density (kg/m^3)	Viscosity (kg/ms)
Air	293	1.225	1.7894×10^{-5}

Each wind turbines were studied with steady simulation at 36 different starting angles from 0º to 360º with 10º increment. Additionally, Model 1 and Model 2 were simulated with transient simulation at 5 different tip speed ratio (TSR) 0.45, 0.5, 0.55, 0.6 and 0.65.

2.3 Experimental Method

To validate the numerical result from the simulations, experiments were conducted. The geometry of the wind turbine models was generated using 3D printing machine. The 3D models were installed inside Taylor's University Wind Tunnel test section to conduct experiment. The wind tunnel consists of rectangular test section, diffuser, contraction section and a Gamma DAQ F/T transducer to collect force and moment data which transfers to the computer. The other specifications of the wind tunnel are shown in Table 4. Figure 8 presents the wind tunnel and the transducer.

Table 4. Taylor's University wind tunnel specifications.

Contraction ratio	Test section cross section (m)	Test section length (m)	Fan diameter (m)
3:4:1	0.303 × 0.303	0.885	0.63

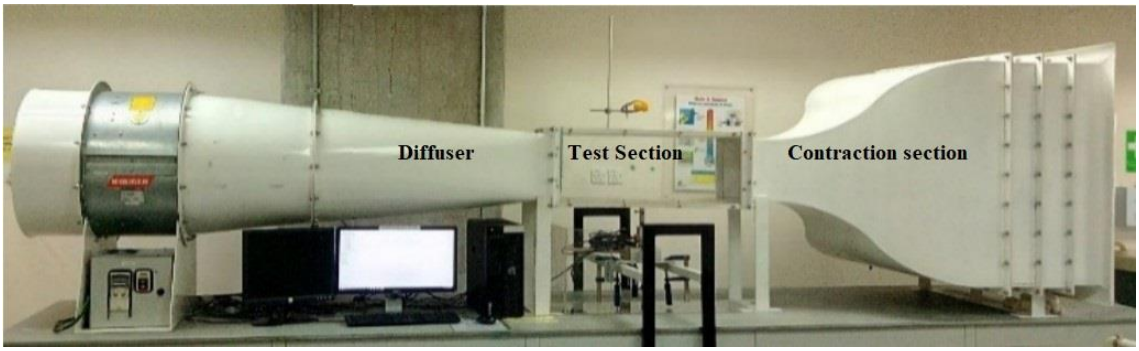

(a)

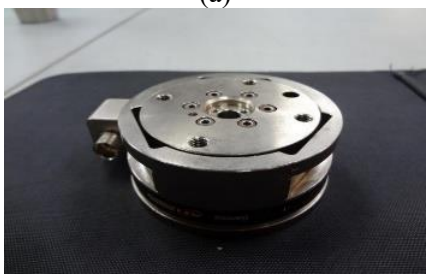

(b)

Figure 8. (a) Taylor's University wind tunnel and (b) ATI GAMMA F/T Transducer [19, 22]

To simplify the work the same dimensions which were used for the numerical simulation were used in order to keep the Reynold number the same. Figures 9 and 10 show the blades for the Darrieus rotors and the Savonius rotors respectively. Figure 11 shows the Base Model assembled. Model 1 and Model 2 were assembled with the same method.

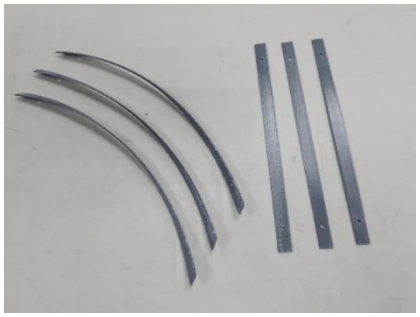

Figure 9. Helical NACA 0015 blades (Left) and Straight NACA 0015 blades (Right)

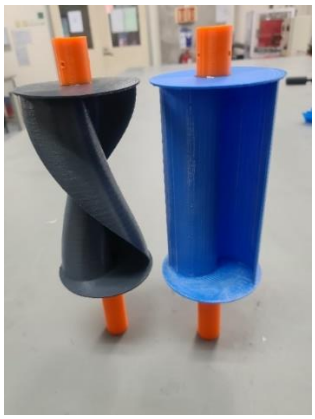

Figure 10. Helical Savonius (Left) and Conventional Savonius (Right)

Figure 11. Model Base assembled

3. Result and Discussion

3.1 Comparison of Wind Turbines at Different Angles

To check the effectiveness of the generated models, Model Base was selected which is a hybrid Savonius-Darrieus VAWT designed and studied by Roshan [21]. Model Base, Model 1 and Model 2 were simulated and experimented at 36 different angles from 0º to 360º. Figures 12 and 13 show the lift and drag coefficient of the wind turbine models on this study at different azimuth angles.

As it can be seen from figure 12 that Model Base has the highest lift coefficient with value of 2.55 at 2 angles while it also has the lowest lift coefficients as well. Between Model Base and Model 2, Model 2 has higher average lift coefficient even though at 10 to 40 degrees and 200 to 220 degrees it has lower lift coefficient compared to Model Base but the difference between the lift coefficients at different azimuth angles it is not as much as the Model Base. This shows that Model 2 has a more stable lift coefficient behavior compared to Model Base. But Model 1 with the highest average lift coefficient of 2.5 has the highest lift coefficient compared to Model Base and Model 2 with an almost stable behavior during the 360 degrees.

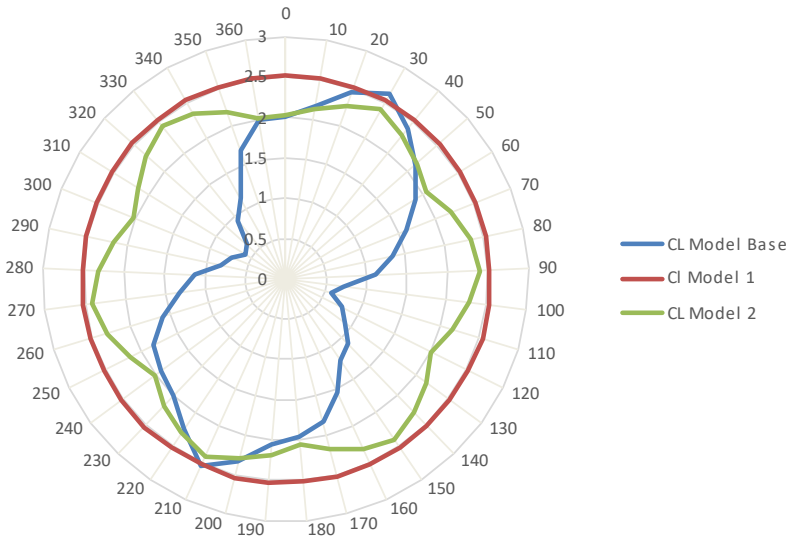

Figure 12. Lift Coefficient of the wind turbine models at different azimuth angle.

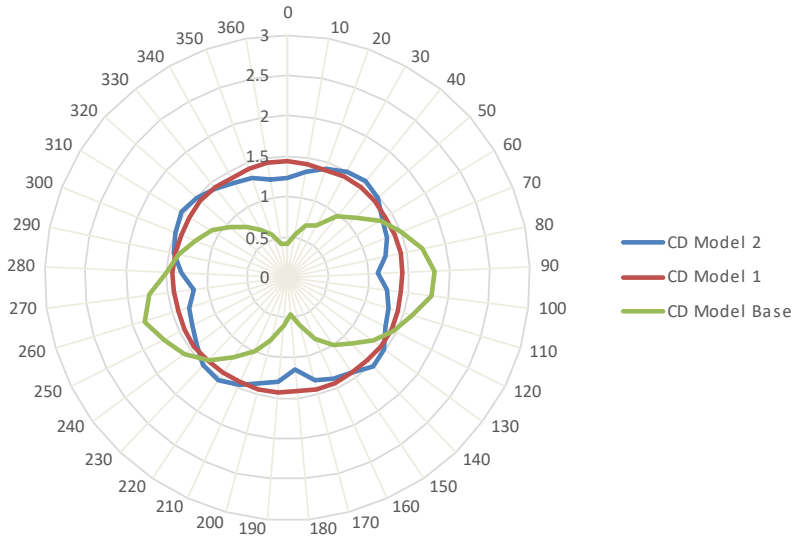

Figure 13. Drag Coefficient of the wind turbine models at different azimuth angle.

Figure 13 shows that the Model Base has the highest drag coefficient between at 70-120 and 235-285 degrees with the maximum drag coefficient of 1.85 and also it achieves the lowest drag coefficient of 0.45 at 0 and 180 degrees. Even though Model 2 achieved higher drag coefficients for four different angle ranges but Model 1, has the highest average drag coefficient with the value of 1.42.

As it's shown in figures 12 and 13, in both lift and drag coefficient, Model 1 has a more stable values at all angles and that is because of the helical design of both Darrieus blades and the Savonius rotor. The design makes the model almost identical at all angles which in result would give a more stable aerodynamic performance compared to Model 2 and Model Base which would be suitable for a wind turbine at low wind speeds.

3.2 Validation of The Numerical Result

To validate the obtained result from the simulations, experiments were conducted. Each model was set in Taylor's wind tunnel test section at 36 different angles from 0 to 360 with 10 degrees increment and obtained their lift and drag force from the experiment. The drag and lift coefficients of each model at the specific angle are calculated using Equations (6) and (7),

$$F_D = C_D A \frac{\rho V^2}{2} \quad (6)$$

$$F_L = C_L A \frac{\rho V^2}{2} \quad (7)$$

where F_D and F_L are drag and lift force respectively and A is the reference area, ρ is the air density, V is the wind velocity and C_D and C_L are the drag coefficient and lift coefficient respectively [25].
Figures 14 and 15 respectively present the obtained result for the lift and drag coefficient for simulations and experiments for the three studied models on this research.

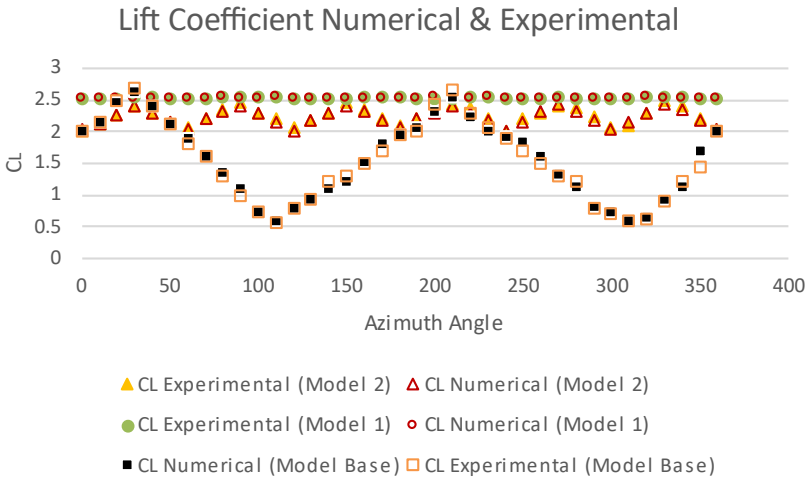

Figure 14. Experimental and numerical result for lift coefficient

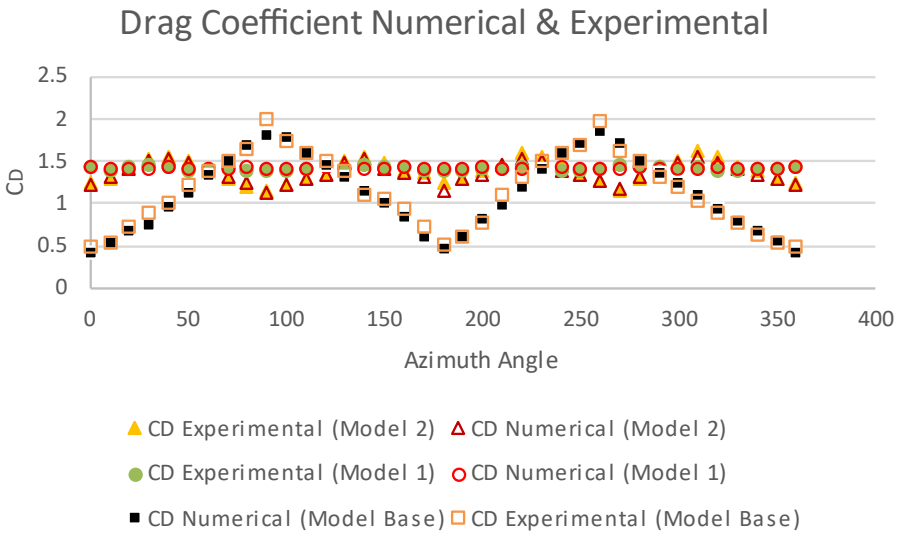

Figure 15. Experimental and numerical result for drag coefficient

As it can be seen on figures 14 and 15, the highest error for the lift coefficient is at 350 degrees which is 14% higher compared to the numerical value. As for the highest error for the drag coefficient, Base Model has 10% higher value at 90 degrees. Yet the difference between the numerical and experimental results for other angles is so small which would validate the selected method for this study.

4. Conclusion

In the presented research, numerical and experimental studies were conducted on three different hybrid Savonius-Darrieus wind turbines. The lift and drag coefficients of the three models at 36 different setting angles were studied and the torque and power coefficient of Model 1 and Model 2 were obtained with the same Reynold's number of 2.5×10^5. The findings of this research are summarized as bellow:

- A hybrid Savonious-Darrieus wind turbine and helical Savonious rotors have a better aerodynamic performance compared to the conventional Savonious rotors at low wind speed.
- In a hybrid Savonious-Darrieus wind turbine, NACA 0015 performs better compared to NACA 0021 as a straight blade at low wind speed.
- In a hybrid Savonious-Darrieus wind turbine, even though straight Darrieus rotors achieve higher power and torque coefficient, but the helical Darrieus blades have a more stable performance which is more suitable for low wind speed.
- Low TSR is more suitable for hybrid Savonius-Darrieus VAWTs at low wind speed.

By having Model 1 to be used for rural schools and clinics, offshore platforms, telecom towers, on or off grid residence at low wind speed locations would reduce the electricity production by power plants and eventually reduce the CO_2 emissions and global warmings.

References

[1] Archer D 2011 *Global Warming: Understanding the Forecast* (Wiley)
[2] Enerdata 2021 Global Energy Statistical Yearbook *Enerdata*
[3] Darkwah W K, Odum B, Addae M, Koomson D, Kwakye Danso B, Oti-Mensah E, Asenso T and Buanya B 2018 Greenhouse Effect: Greenhouse Gases and Their Impact on Global Warming *J. Sci. Res. Reports* **17** 1–9
[4] IEA 2021 Electricity Information *IEA*
[5] Bove R, Bucher M and Ferretti F 2012 Integrating large shares of wind energy in macro-economical cost-effective way *Energy* **43** 438–47
[6] A. Albani M Z I 2013 Preliminary Development Of Prototype Of Savonius Wind Turbine For Application In Low Wind Speed In Kuala Terengganu, Malaysia *Int. J. Sci. Technol. Res.* **2** 102–8
[7] Salih S, Sohif M, Sopian K, Saleh E and M. A 2014 Simulation analysis of Venturi-Vertical Axis Wind Turbine (V-VAWT)
[8] Nemes C and Munteanu F 2010 Optimal selection of wind turbine for a specific area *Proceedings of the International Conference on Optimisation of Electrical and Electronic Equipment, OPTIM* pp 1224–9
[9] Sarkar A and Behera D K 2012 Wind Turbine Blade Efficiency and Power Calculation with Electrical Analogy *Int. J. Sci. Res. Publ.* **2** 1–5
[10] Sørensen J N 2011 Aerodynamic Aspects of Wind Energy Conversion *Annu. Rev. Fluid Mech.* **43** 427–48
[11] Tong W 2011 *Wind Power Generation and Wind Turbine Design* ed W Tong (WIT Press)
[12] Liang X, Fu S, Ou B, Wu C, Chao C Y H and Pi K 2017 A computational study of the effects of the radius ratio and attachment angle on the performance of a Darrieus-Savonius combined wind turbine *Renew. Energy* **113** 329–34
[13] Jeon K S, Jeong J I, Pan J-K and Ryu K-W 2015 Effects of end plates with various shapes and sizes on helical Savonius wind turbines *Renew. Energy* **79** 167–76

[14] Micha Premkumar T, Sivamani S, Kirthees E, Hariram V and Mohan T 2018 Data set on the experimental investigations of a helical Savonius style VAWT with and without end plates *Data Br.* **19** 1925–32
[15] Saha U K, Thotla S and Maity D 2008 Optimum design configuration of Savonius rotor through wind tunnel experiments *J. Wind Eng. Ind. Aerodyn.* **96** 1359–75
[16] Ahmed Y, Hassanzadeh R, Yaakob O and Ismail M 2013 Comparison of Conventional and Helical Savonius Marine Current Turbine Using Computational Fluid Dynamics *World Appl. Sci. J.* **28** 1113–9
[17] Mayeed M 2014 Designing Wind Turbines for Areas With Low Wind Speeds *Am. Soc. Mech. Eng. Fluids Eng. Div. FEDSM* **1**
[18] Deo A, Goundar J, Narayan S and Chettiar N 2015 Design and Performance Analysis of Micro Wind Turbine for Fiji *Int. J. Inf. Electron. Eng.* 37–40
[19] Nongdhar D and Goswami B 2018 Design of Micro Wind Turbine for Low Wind Speed Areas: a Review *ADBU J. Electr. Electron. Eng.* **2** 36–41
[20] Battisti L, Brighenti A, Benini E and Castelli M 2016 Analysis of Different Blade Architectures on small VAWT Performance *J. Phys. Conf. Ser.* **753** 62009
[21] Roshan A, Sagharichi A and Maghrebi M 2019 Nondimensional Parameters' Effects on Hybrid Darrieus- Savonius Wind Turbine Performance *J. Energy Resour. Technol. Trans. ASME* **142**
[22] Eftekhari S and Al-Obaidi A S 2019 Investigation of a NACA0012 Finite Wing Aerodynamics at Low Reynold's Numbers and 0º to 90º Angle of Attack *J. Aerosp. Technol. Manag.* **11**
[23] Mohamed M H, Ali A M and Hafiz A A 2015 CFD analysis for H-rotor Darrieus turbine as a low speed wind energy converter *Eng. Sci. Technol. an Int. J.* **18** 1–13
[24] Chawla S, Chauhan A and Bala S 2015 Parametric study of hybrid Savonius-Darrieus turbine *2015 2nd International Conference on Recent Advances in Engineering Computational Sciences (RAECS)* pp 1–5
[25] Eftekhari H, Al-obaidi A S M and Eftekhari S 2020 THE EFFECT OF SPOILER SHAPE AND SETTING ANGLE ON RACING CARS AERODYNAMIC PERFORMANCE *Indones. J. Sci. Technol.* **5** 11–20